

NONSTEADY-STATE MODEL OF DOUBLE POROSITY FOR THE CONSIDERATION OF RADIONUCLIDES' MIGRATION AT THE "ENISEYSKIY" SITE

Vasilyev A. D., Kondratenko P. S., Matveev L. V.

Nuclear Safety Institute of RAS, Moscow

The article was received on 7 December 2017.

The results of development of numerical and analytical methods and their application to radionuclides transport following safety barriers failure in the vicinity of disposal facility at "Eniseyskiy" site of Nizhnekansk massif are presented in the paper. The analysis includes numerical modeling and analytical asymptotic evaluation on the basis of two-porous medium model which is supposed to be the most adequate for numerical migration analysis considering the hydrogeological conditions at the "Eniseyskiy" site.

Preliminary assessments (taking into account currently available information on key environment parameters) lead to a conclusion that radionuclides (with low sorption capability) will reach the Enisey River in time of the order $3 \cdot 10^5 - 1 \cdot 10^6$ years. Correspondingly, this time will be even longer for the radionuclides with high sorption ability by a factor of R where R is the retardation factor due to sorption, meaning that only isotopes with very long decay half-lives will reach the daylight surface. This conclusion indicates that the levels of radiation effect on the environment would be insignificant.

Keywords: Numerical modeling, analytical model, diffusion, migration of particles, radioactive waste disposal, radionuclides

Introduction

Realistic forecasting of radionuclide transport in the geological environment in the vicinity of the designed deep radioactive waste disposal facility at the "Eniseyskiy" site at the Nizhnekansk massif is a key factor for long-term safety case of the facility.

The most probable admixture migration pathway is their transport with filtration flow of ground waters discharged in the western direction to the under-riverbed flow of the Enisey River [1] (Fig. 1, 2). There is also a certain probability that the transport will have Northeastern direction towards the Shumikha River, a tributary of the Enisey.

It is assumed that the main transport mechanism in the granitoid rock mass (Archaen gneiss) would be advection along fractures in the rock with diffusion to the blocks neighbouring the fractures.

Nizhnekansk massif is characterized by slow water exchange rates. Water is exchanged along several fracture systems [1]. Assessment of water particle lifetime in process of its movement with the flow of

groundwater from deep radioactive waste disposal facility to riverbed gives values of approximately 25 000 years, as discussed in section 2.2. Therefore, average advection rate is low, thus contributing to low migration rate and late release of radionuclides to daylight surface.

A number of calculations of radionuclides transport from the "Eniseyskiy" site of Nizhnekansk massif using various analytical or numerical instruments have been already completed or are currently being underway.

For example, the results of calculation of radionuclide migration along their propagation pathway from the deep disposal facility to the daylight surface using GoldSim code were presented in the report [1]. According to these results, maximum value of radionuclide flow to the environment would be reached within $10^4 - 10^5$ years depending on radionuclide type.

Admixture transport in two-porous environments is usually described [2] by models where admixture

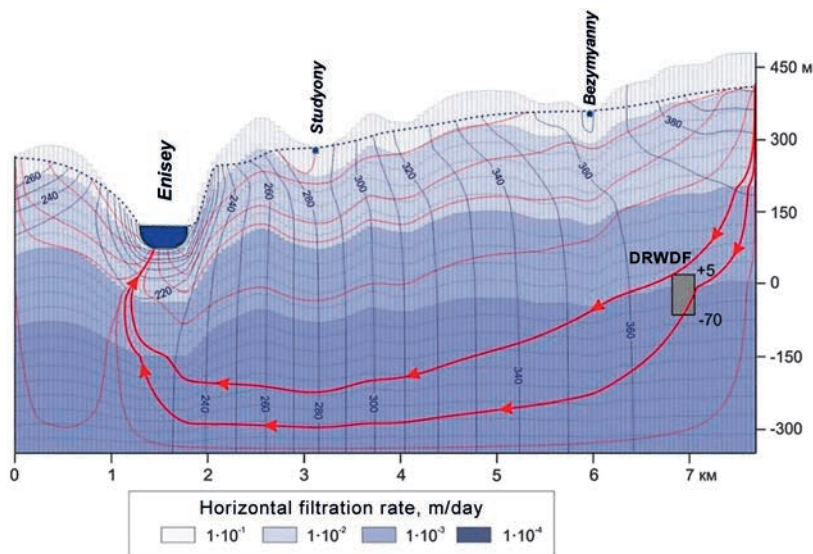


Fig. 1. Groundwater flow line in the vertical plane in the vicinity of the deep radioactive waste disposal facility at the "Eniseyskiy" site

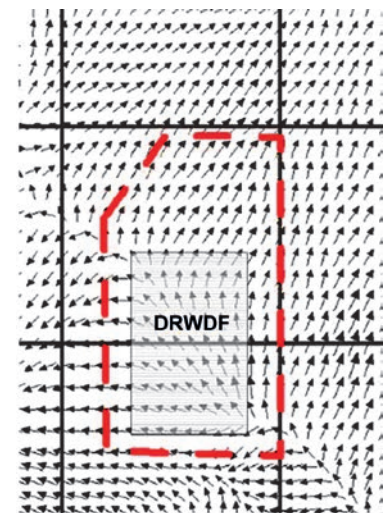


Fig. 2. Groundwater flow line in the horizontal plane in the vicinity of the deep radioactive waste disposal facility at the "Eniseyskiy" site

fractions concentrated in well permeable channels and weakly permeable porous blocks are described by mean concentrations averaged at scales exceeding the characteristic dimensions of these blocks. In this case, the exchange rate between the subsystems is taken to be proportional to the difference of these mean concentrations [3, 4]. This provides a good approximation for description of the most of admixture mass at large time scales, when concentration gradients at individual blocks may be neglected. Nevertheless, if the block dimensions are substantially large, the time of concentration equalization may also be large, leading to substantial role of the described gradients in description of system dynamics. Direct numerical modeling of transport in a slow medium is possible, however, it requires considerable calculation efforts, while important asymptotic features of the transport process will remain unidentified.

A non-steady model of sharply contrasting two-porous medium with concentration behaviour described by integral-differential equation [9] was developed to avoid these drawbacks. Numerical model based on the one described above and the developed effective algorithm for integral kernel calculation have been applied in the current paper to radionuclide transport processes at "Eniseyskiy" site. One of the conclusions of the study was that the actual admixture transportation rate at large time vales was further reduced compared to advection rate due to removal of particles from the fast environment to dense matrix. Therefore, the actual rate of admixture migration is reduced by several orders of magnitude compared to groundwater filtration rate and radionuclide release time (even for nuclides with low sorption capability, not mentioning the strongly adsorbed isotopes) to the Enisey River turns out to be very high, — $3 \cdot 10^5 - 1 \cdot 10^6$ years.

1 Development of calculation algorithm for description of non-classical transport processes for a model with sharply contrasting statistically uniform environment

Multiple studies of admixture migration in sharply heterogeneous environments performed over the last decades had demonstrated mostly non-classical character of particles transport [5–9]. For fracture-porous environments characteristic for the Nizhnekansk massif, the uniform porosity approximation is insufficient. In this case, the description should be based on the double porosity model (or in other words, the model of two-porous environment), when the system is considered as a superposition of two subsystems (Fig. 3):

- well permeable channels (usually corresponding to fracture networks);
- weakly permeable blocks filling the space between the channels (fractures).

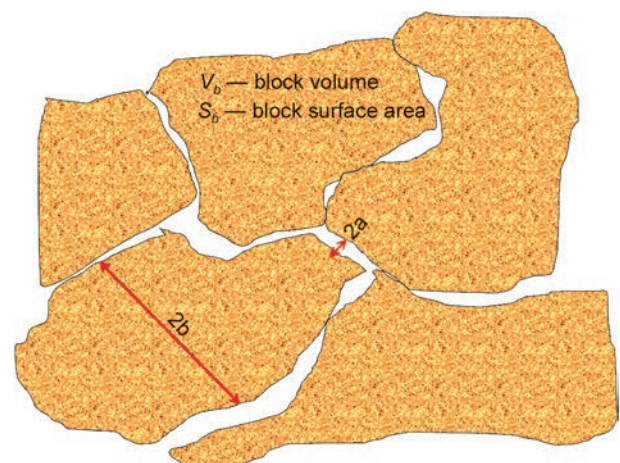


Fig. 3. Two-porous environment model: 2a – aperture of channels, 2b – characteristic diameter of units

Generally, for various environments the aperture of channels 2a may vary in the wide range from 10⁻⁶ to 10⁻² m, while the dimensions of blocks 2b change in the range of 10⁻¹ to 10¹ m. The block dimension is a value of the order of the characteristic distance between the fractures. These data were obtained out of analysis of works on this topic (see, e.g., [10, 11]).

There are various methods for numerical simulation of admixture transport in such sharply contrasting geological environments, based on relevant mathematical models of these processes. The approach suggested below is based on the use of exact analytical solutions of diffusion equation in a weakly permeable environment with a simultaneous solution of diffusion and advection equations in a well permeable (fast) environment.

1.1 Numerical implementation of double porosity model for description of non-classical (non-equilibrium) transport

Let us consider single-dimension diffusion and advection problem for a system shown in Fig. 4.

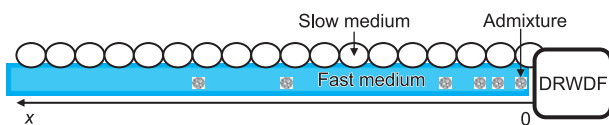


Fig. 4. Geometry of admixture migration problem in sharply contrasting geological environment

Active admixture concentration equation (admixture in fast environment) was considered as the initial equation in development of calculation algorithm for description of non-classical transport processes for a model with sharply contrasting statistically uniform medium:

$$\frac{\partial c(\vec{r}, t)}{\partial t} + \vec{u} \cdot \vec{\nabla} c - D \Delta c(\vec{r}, t) = q(\vec{r}, t) - \lambda c(\vec{r}, t). \quad (1)$$

Here $c(\vec{r}, t)$ – volumetric or mass concentration of admixture particles, 1/m³ or kg/m³;
 $\vec{r} = (x, y, z)$ – spatial coordinate, m;
 t – current time, s;
 \vec{u} – average advection rate, m/s;
 D – particle diffusion coefficient in fast environment (water), m²/s;
 $\lambda = 0.693/T_{1/2}$ – power index for isotope decay curve, T_{1/2} – half-life period;
 $q(\vec{r}, t)$ – admixture exchange between slow and fast environments (source), 1/(m³·s) or kg/(m³·s).

Below we will not take into account the last component in the right hand side of (1) in analytical analysis, but it will be taken into account in conclusions.

Generally, there would be particle sink from the fast environment to the slow one, therefore the variable q would be negative in most cases (below

zero), i.e. the number of particles in the fast environment would reduce with time.

Nevertheless, a situation is possible when after the passing of the main wave, the admixture concentration in the blocks will exceed the concentration in the channel (i.e. in the fast environment). Then there would be reverse flow of admixture from the slow environment to the fast one ($q > 0$). Thus, the model takes into account exchange of admixture between the fast and slow subsystems in both direct and reverse directions.

Water diffusion coefficient for most admixtures varies in the range of 10⁻⁸ – 10⁻¹⁰ m²/s.

The source $q(\vec{r}, t)$ may be written as:

$$q(\vec{r}, t) = - \frac{\partial}{\partial t} \int_0^t dt' \varphi(t-t') c(\vec{r}, t') = - \frac{\partial}{\partial t} \int_0^t dt' \varphi(t') c(\vec{r}, t-t'), \quad (2)$$

i.e. as a derivative with respect to time of a “contraction” type integral. Construction of the function $\varphi(t)$ (integral kernel), describing admixture sink to weakly permeable blocks is an important element of the theory.

In the general case such blocks may have an arbitrary form and there could be a significant scatter in their dimensions, therefore the exact equation for $\varphi(t)$ cannot be constructed. Nevertheless, for time intervals important for description of admixture concentration (in particular, for the interval with non-classical behaviour) the function has well-defined asymptotics independent of block forms and defined only by mean environment parameters:

- V_b – average block volume, m³;
- S_b – surface area of a single block, m²;
- d – particle diffusion coefficient in slow environment, m²/s;
- R – admixture retardation coefficient for the blocks in equilibrium sorption model, dimensionless units;
- φ_b – porosity of the blocks (volumetric fraction of cavities), dimensionless units;
- φ_{fr} – volumetric fraction of mobile areas, dimensionless units.

Then the characteristic time for the admixture transferred to the block to become equal to the quantity of admixture in the channel may be determined as:

$$t_a = \left(\frac{V_b}{S_b A} \right)^2 \frac{1}{dR}. \quad (3)$$

On the other hand, the characteristic time of admixture spreading in the block is assessed as:

$$t_b = \left(\frac{V_b}{S_b} \right)^2 \frac{R}{d}. \quad (4)$$

Parameter A is the ratio of block porosity to fractures (volumetric fraction taken by mobile subareas):

$$A = \varphi_b / \varphi_{fr}. \quad (5)$$

As $\varphi_b \sim 5 \cdot 10^{-3} - 5 \cdot 10^{-1}$, and $\varphi_{fr} \sim a/b \ll 10^{-2}$ (a – characteristic fracture width, $b \approx V_b/S_b$ – characteristic block dimension), then for nearly all practically important cases $A \gg 1$ and, respectively, time $t_a \ll t_b$. Assuming that admixture is not adsorbed ($R = 1$), the parameter t_a/t_b is simply equal to $1/A^2$, i.e. is completely determined by geometric characteristics of the environment. Detailed overview of adsorption behaviour of admixtures in fracture-porous environments with account for hysteresis is given in [4]. In accordance with this work, the retardation parameter R may vary within an order of magnitude $R \approx 1 - 16$ depending on the radionuclide. Out of (3), (4) it can be concluded that the higher the R , the lower the ratio t_a/t_b .

The ratio of characteristic times t_a/t_b is an exceptionally important parameter of the system as would be demonstrated below. This value would ultimately determine the key output parameters of the problem: radionuclide concentrations in output points and time of radionuclide release to daylight surface.

Let us consider measurement of the diffusion coefficient d in the slow environment in more detail.

In a uniform environment (e.g., in water solution), the admixture mass flow is described by the classic Ficks law:

$$J = -D \frac{\partial c}{\partial x}, \quad (6)$$

where J – admixture mass flow in the x axis direction, $\text{kg}/(\text{m}^2\text{s})$; D – diffusion coefficient, m^2/s ; c – admixture mass concentration, kg/m^3 .

The geological environment of Nizhnekansk massif is fracture-porous, with fractures and pores completely or partially (in the aeration zone) filled with water. For fracture-porous environment the flow equation (6) is transformed as follows:

$$J = -\frac{\varepsilon s D}{T_m} \frac{\partial c}{\partial x}, \quad (7)$$

where ε – porosity, s – saturation (volumetric water fraction in fractures and pores), T_m – fracture and pore curve factor. The curve factor is calculated using:

$$T_m = \left(\frac{l_{eff}}{l} \right)^2, \quad (8)$$

where l – distance between two points in a straight line x , l_{eff} – actual length of the particle migration path with account for curvilinear open pores. Parameter T_m is equal to several units.

The equation (7) may be written as

$$J = -D_{eff} \frac{\partial c}{\partial x}, \quad D_{eff} = \frac{\varepsilon s D}{T_m}. \quad (9)$$

As diffusion takes place only in water environment in fractures and pores, and the environment in the vicinity of the disposal facility is saturated ($s = 1$), then the value of diffusion coefficient d in the slow environment in terms of characteristic times t_a (3) and t_b (4), has the form of:

$$d = \frac{D}{T_m}, \quad (10)$$

i.e. is several times lower than the diffusion coefficient in water (curvilinear factor).

Let us continue the analysis of transport in two-porous environment. The integral kernel $\varphi(t)$ in equation (2) may be approximately represented in the following forms for small ($t \ll t_b$):

$$\varphi(t) \approx \frac{1}{\sqrt{t_a t_b}} \left[-1 + \sqrt{\frac{t_a}{\pi t_b}} \left[1 + 2 \sum_{n=1}^{\infty} \exp\left(-n^2 \frac{t_b}{t_a}\right) \right] \right] \quad (11)$$

and large ($t \gg t_b$) time values:

$$\varphi(t) \approx \frac{2}{\sqrt{t_a t_b}} \sum_{n=1}^{\infty} \exp\left[-(n\pi)^2 \frac{t}{t_b}\right]. \quad (12)$$

Let us approximate the integrals in (2) as follows:

$$\begin{aligned} \Phi_l &= \int_{(l-1)\tau}^{l\tau} dt' \varphi(t') = \\ &= \frac{\tau}{\sqrt{t_a t_b}} \left(2 \sqrt{\frac{t_b}{4\pi\tau}} \left(\sqrt{l} - \sqrt{l-1} \right) - 1 \right), \quad l \leq \frac{t_b}{6\tau} \quad (13) \end{aligned}$$

$$\begin{aligned} \Phi_l &= \int_{(l-1)\tau}^{l\tau} dt' \varphi(t') = \\ &= \frac{2}{\pi^2} \sqrt{\frac{t_b}{t_a}} \left[\exp\left(\frac{\pi^2 \tau}{t_b}\right) - 1 \right] \exp\left(-\frac{\pi^2 \tau}{t_b} l\right), \quad l > \frac{t_b}{6\tau}. \quad (14) \end{aligned}$$

The following numerical scheme was applied for numerical calculation of equation (1) in 1D approximation:

$$\begin{aligned} &\frac{1}{\tau} \left[c_i^n - c_i^{n-1} + \sum_{l=1}^{n-1} \Phi_l c_i^{n-l+1} - \sum_{l=1}^{n-1} \Phi_l c_i^{n-l} \right] - \\ &- \frac{D}{h^2} \left[s \Lambda_i^n + (1-s) \Lambda_i^{n-1} \right] = 0, \quad (15) \end{aligned}$$

where operator Λ_i^n is equal to:

$$\Lambda_i^n = c_{i+1}^n - 2c_i^n + c_{i-1}^n. \quad (16)$$

The following symbols are used in equation (15):
 τ – time step, s;
 h – spatial discretization step, m;
 D – diffusion coefficient in fast environment, m²/s;
 s – implicitness parameter of the numerical scheme, dimensionless units.
 The upper index indicated the time step number ($0 < n < N$), the lower index – number of spatial step ($0 < i < M$).

The system was resolved by two methods: Gaussian methods for rarefied matrices and fitting method. Both methods gave the same results.

1.2 Comparison of the results of numerical modeling of Q-diffusion and Q-advection with analytical asymptotics

Diffusion. Let us assign the boundary conditions in the following form. The flow at the left hand side and right hand side borders of the fast environment (Fig.4) is equal to zero. Advection rate is also equal to zero, i.e. $\bar{u} = 0$. The particles sink from the fast environment to the slow one. Sorption is taken into account in parameters t_a and t_b , see expressions (3) and (4).

Initial conditions. At the initial time moment the particles were present in the first 10 calculation cells (each calculation cell had dimensions $h = 0.05$ m), where the concentration was such ($c_0 = 2$), that concentration integral with respect to x was equal to 1 (as for δ -function), i. e. there was only one particle in the system $N_0 = 1$. Concentration in all other cells was equal to 0.

Neglecting the decay (eternal half-life period $T_{1/2}$), the number of particles in the fast environment N_1 may be assessed analytically. Thus, the number of particles in the mobile subsystem reduces with time in accordance with the following law:

$$N \approx N_1 = N_0 \sqrt{\frac{t_a}{\pi t}}, \quad t_a \ll t \ll t_b, \quad (17)$$

$$N \approx N_2 = N_0 \sqrt{\frac{t_a}{\pi t_b}}, \quad t \gg t_b. \quad (18)$$

At small distances from the initial admixture position (integral kernel, near field) the following asymptotics F_0 would be true:

$$c(x,t) \approx F_0(x,t), \quad x \ll \sqrt{D\sqrt{t_a t}}, \quad (19)$$

$$F_0(x,t) = \frac{N_1}{\sqrt{D\sqrt{t_a t}}} \frac{\sqrt{\pi}}{2\Gamma(\frac{1}{4})} \left[1 + \frac{\Gamma(\frac{1}{4})}{8\Gamma(\frac{3}{4})} \sqrt{\frac{t_a}{t}} - \alpha^2 \frac{\Gamma(\frac{1}{4})}{8\Gamma(\frac{3}{4})} \right], \quad (20)$$

where t – time, s; x – coordinate, m; $\Gamma(\xi)$ – gamma-function.

Parameter α is equal to

$$\alpha = \sqrt{\frac{x^2}{D\sqrt{t_a t}}}. \quad (21)$$

For large distances $1 \ll \alpha \ll 4(t/t_a)^{3/4}$ (near-field tail of distribution) the following F_1 asymptotics would be true:

$$c(x,t) \approx F_1(x,t), \quad 1 \ll \alpha \ll 4\left(\frac{t}{t_a}\right)^{3/4}, \quad (22)$$

$$F_1(x,t) = \frac{N_0}{\sqrt{6\pi Dt}} \left[\frac{t_a}{t} \left(\frac{\alpha}{4}\right)^{4/3} \right]^{1/4} \exp \left[-3 \left(\frac{\alpha}{4}\right)^{4/3} \right]. \quad (23)$$

Fig. 5–8 show numerical solutions for admixture concentration distribution dependent on the node number (lengthwise coordinate) for various time moments, and for various environment parameters t_a and t_b . Asymptotics F_0 and F_1 for the near field and near tail respectively are given in all graphs.

Fig. 5 shows the concentration profile for time moment $t = 10^7$ s. Initial concentration was equal to $c_0 = 2$ in the first 10 cells. It can be seen that particle concentration drop in the absence of particle sink to the slow environment (results marked as No sink) by this time is not significant compared to initial concentration and proceeds due to diffusion washing out. However, in the presence of particle transfer from the fast to the slow environment, as it happens in reality, the number of particles in the fast environment drops rapidly.

The curves given in the figure show that identical results were obtained for different methods of equations system solution and for different time step values.

Fig. 5 and 6 also demonstrate that the envelope of asymptotics F_0 and F_1 slightly underestimates the exact solution of the problem. This factor is explained by the fact that in the initial distribution in calculations the particles were present in the first 10 cells, while asymptotics F_0 and F_1 were obtained out of an assumption that the initial distribution has the form of a δ -function.

Overall, Fig. 5–8 show reasonable behaviour of admixture concentration in the near field and in the near tail (i.e. in the areas where the radionuclide concentrations are equal to or above the maximum allowed levels), and the fact that asymptotics F_0 and F_1 may be successfully used for express assessment of particle concentrations. In order to verify the hypothesis about deviation of numerical and asymptotic solutions caused by deviation of initial distribution from the δ -function, Fig. 7 shows numerical solutions for initial particle distribution not in the first 10 cells, but in the first two cells. It can be seen, that numerical results and the envelope of asymptotics F_0 and F_1 show much better agreement. In particular, asymptotics F_1 virtually coincides with the exact solution in the range of coordinates

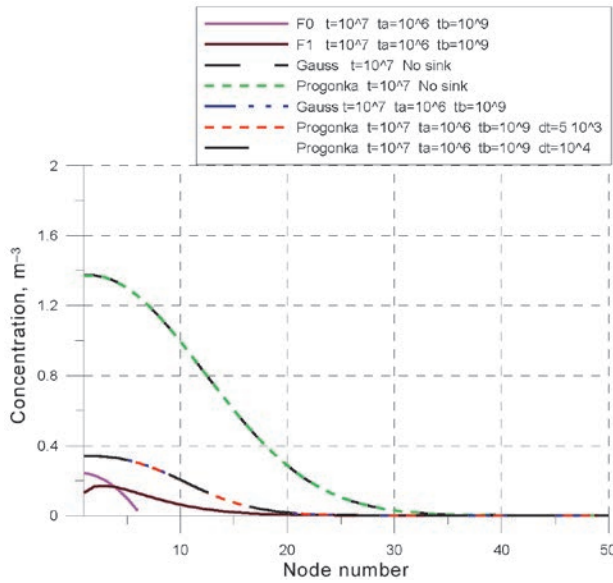


Fig. 5. Concentration distribution profile for time moment $t = 10^7$ s ($t_a = 10^6$ s and $t_b = 10^9$ s). Asymptotics F_0 and F_1 are shown

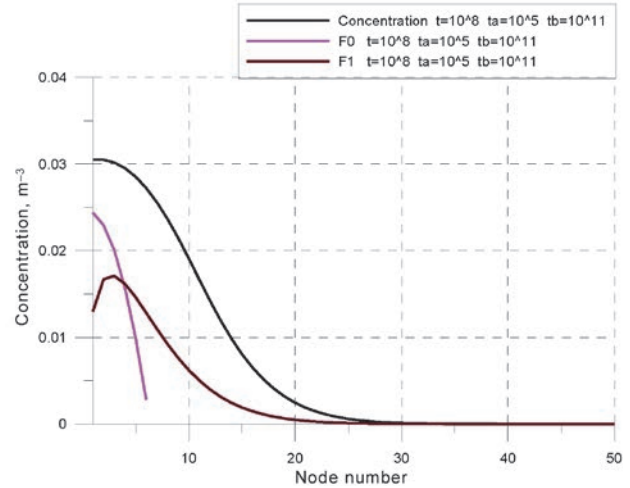


Fig. 6. Concentration distribution profile for time moment $t = 10^8$ s ($t_a = 10^5$ s and $t_b = 10^{11}$ s). Asymptotics F_0 and F_1 are shown

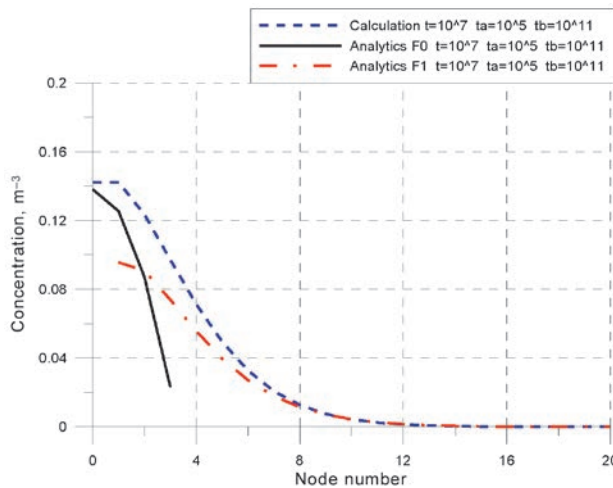


Fig. 7. Concentration distribution profile for time moment $t = 10^7$ s ($t_a = 10^5$ s and $t_b = 10^{11}$ s). Asymptotics F_0 and F_1 approximating the numerical solution are shown

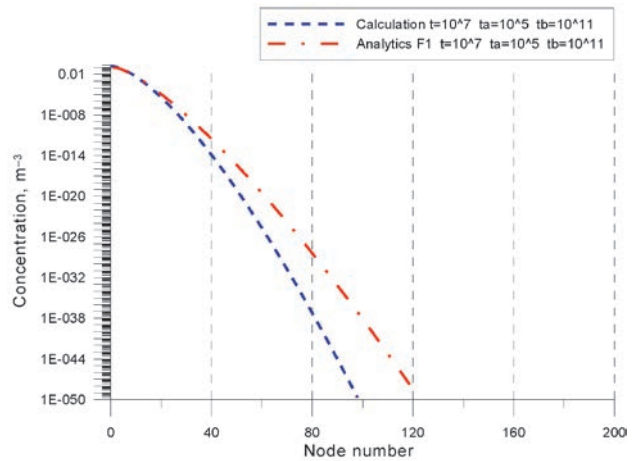


Fig. 8. Concentration distribution profile in logarithm scale for time moment $t = 10^7$ s ($t_a = 10^5$ s and $t_b = 10^7$ s). Asymptotics F_1 approximating numerical solution in the near tail is shown

corresponding to the near tail. This is an additional factor in favor of extensive forecasting capabilities of the approximations obtained.

Fig. 8 shows distribution of particle concentrations in logarithmic scale. The figure shows that asymptotics F_1 works well in the near tail, whilst in the far tail it deviates from the true solution of the problem.

Let us consider particle number concentration in the system. The numerical scheme applied to the solution of equations system ensures particle number conservation in both the fast and slow environments. However, it is interesting to consider the issue of number of particles in the fast subsystem, which shall satisfy the asymptotic solution (17) at large time scales. Table 1 lists calculation

and analytical values for particle numbers in the fast environment N for various time moments and input parameters.

Table 1. Number of particles in the fast environment in case of diffusion transport

Calculation parameters	$t=10^8$ c $t_a=10^6$ c $t_b=10^{10}$ c	$t=10^7$ c $t_a=10^6$ c $t_b=10^9$ c	$t=10^7$ c $t_a=10^5$ c $t_b=10^{11}$ c	$t=10^8$ c $t_a=10^5$ c $t_b=10^{11}$ c	$t=10^9$ c $t_a=10^5$ c $t_b=10^{11}$ c
N_1 analytical	$5.65 \cdot 10^{-2}$	0.179	$5.65 \cdot 10^{-2}$	$1.79 \cdot 10^{-2}$	$5.65 \cdot 10^{-3}$
N_1 calculation	$6.04 \cdot 10^{-2}$	0.179	$5.32 \cdot 10^{-2}$	$1.70 \cdot 10^{-2}$	$5.52 \cdot 10^{-3}$

Table analysis shows that the analytical relation (17) is in good agreement with the numerical value (area under the distribution curve). This means that the ratio may be successfully used for express assessment of the number of particles in the mobile subsystem.

Advection. In this case it is assumed that only transport of particles in liquid phase (advection) is present in the fast (mobile) subsystem, and there is no diffusion (equation 1). There still is a sink of particles from the fast environment to the slow one. In the approximation of eternal half-life $T_{1/2}$ the result is:

$$\frac{\partial c}{\partial t} + u \frac{\partial c}{\partial x} = q. \tag{24}$$

In this case the equation system has the following approximate solution for the near distribution tail:

$$c \approx F_2(x, t), \quad t_a \ll t \ll t_b, \tag{25}$$

$$F_2(x, t) = \frac{x}{u\tilde{t}\sqrt{4\pi D_u\tilde{t}}} \exp\left(-\frac{x^2}{4D_u\tilde{t}}\right), \tag{26}$$

$$\tilde{t} = t - \frac{x}{u}, \quad D_u = u^2 t_a. \tag{27}$$

Fig. 9–11 show the results for an initial distribution with particles present only in the 11-th and 12-th cells. The initial distribution was shifted 10 cells to the right with respect to the beginning of coordinates to provide easy comparison with asymptotics F_2 , which corresponded to the initial distribution in the form of a δ -function at the zero x coordinate. The integral of the initial particle distribution was still equal to one.

Results show good agreement between the numerical calculations and asymptotics F_2 , which shows best fit for fairly large times.

Fig. 9, 10 demonstrate admixture transport in case of particles sink to the slow environment. It can be seen that the area under the distribution curve drops with time, thus indicating the decrease of particle number in the mobile subsystem.

Fig. 11 shows distribution of particles for various time moments in logarithmic scale, derived from asymptotics F_2 . It can be observed that distribution becomes smoother with time, while concentration values in the near field and near tail of the distribution are ever-decreasing.

Table 2 shows comparison of particle number in the mobile subsystem obtained from the numerical solution and asymptotics F_2 . Again, there is a good agreement of particle numbers N for various time moments and input parameters for both methods.

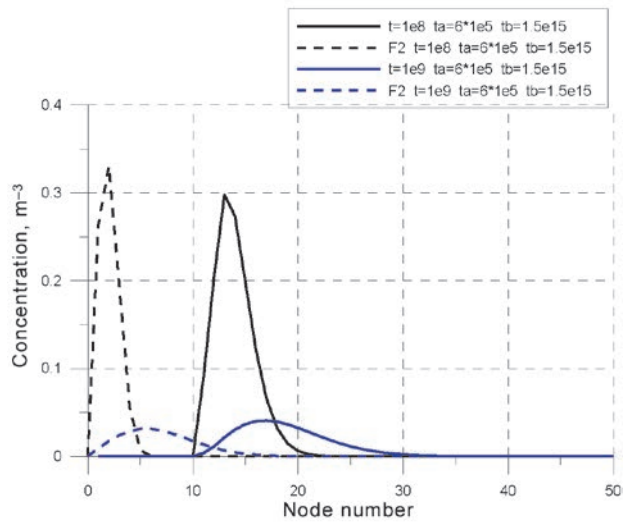


Fig. 9. Concentration distribution profile for time moments $t = 10^8$ s and 10^9 s ($t_a = 6 \cdot 10^5$ s and $t_b = 1.5 \cdot 10^5$ s). Advection rate $u = 8 \cdot 10^{-9}$ m/s

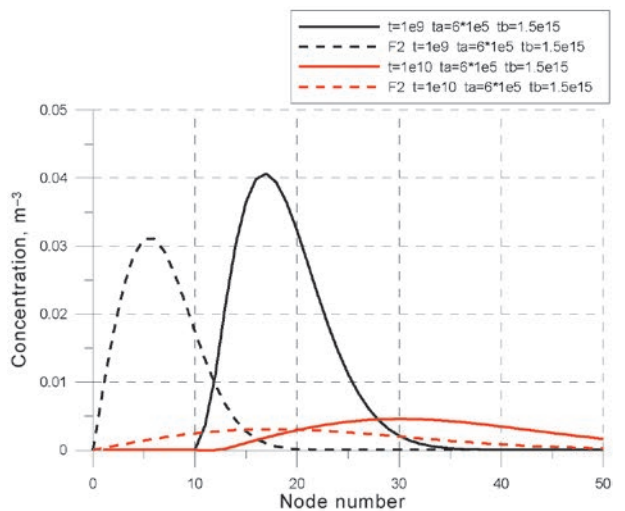


Fig. 10. Concentration distribution profile for time moments $t = 10^9$ s and 10^{10} s ($t_a = 6 \cdot 10^5$ s and $t_b = 1.5 \cdot 10^{15}$ s). Asymptotics F_2 is shown. Advection rate $u = 8 \cdot 10^{-9}$ m/s

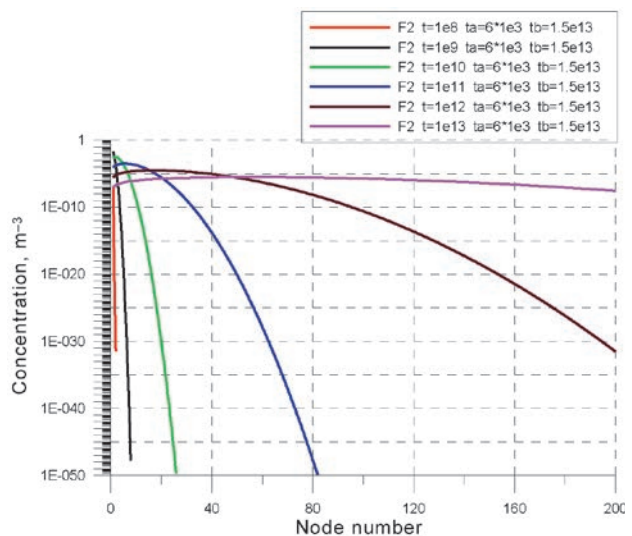


Fig. 11. Asymptotic concentration distribution profile in logarithm scale for time moments $t = 10^8$ s, 10^9 s, 10^{10} s, 10^{11} s, 10^{12} s, 10^{13} s. Parameters $t_a = 6 \cdot 10^5$ s and $t_b = 1.5 \cdot 10^{15}$ s. Advection rate $u = 8 \cdot 10^{-9}$ m/s

Table 2. Number of particles in the fast environment in case of advection transport

Calculation parameters	$t=10^5$ c $t_a=6 \cdot 10^3$ c $t_b=1.5 \cdot 10^{13}$ c	$t=10^6$ c $t_a=6 \cdot 10^3$ c $t_b=1.5 \cdot 10^{13}$ c	$t=10^7$ c $t_a=6 \cdot 10^3$ c $t_b=1.5 \cdot 10^{13}$ c	$t=3 \cdot 10^7$ c $t_a=6 \cdot 10^3$ c $t_b=1.5 \cdot 10^{13}$ c	$t=10^8$ c $t_a=6 \cdot 10^3$ c $t_b=1.5 \cdot 10^{13}$ c
N_1 analytical	0,138	$4,37 \cdot 10^{-2}$	$1,38 \cdot 10^{-2}$	$7,98 \cdot 10^{-3}$	$4,37 \cdot 10^{-3}$
N_1 calculation	1.10	$4.78 \cdot 10^{-2}$	$1.52 \cdot 10^{-2}$	$8.79 \cdot 10^{-3}$	$4.82 \cdot 10^{-3}$

Advection+diffusion. Analytical assessment of long-range radionuclide migration (up to Enisey and Shumikha Rivers) will require the knowledge of asymptotics of the far distribution tail for the combined advection+diffusion problem.

Another characteristic time is used in this problem:

$$t_u = \frac{4D}{u^2}, \quad (28)$$

where u - advection rate.

Applying assessments, we will get $t_u \approx 4 \cdot 10^{-9} / (8 \cdot 10^{-9})^2$ c $\approx 6.2 \cdot 10^7$ s. Let us assess the dimensionless parameter $t_u^2 / (t_a t_b)$ for the geological formation of "Eniseyskiy" section. If $t_a \sim 10^7$ s, and $t_b \sim 10^{11}$, then $t_u^2 / (t_a t_b) \approx 3,6 \cdot 10^{-3}$.

For $t_u^2 / (t_a t_b) \ll 1$ the following asymptotics are true:

$$c(x, t) \approx \frac{N_0}{\sqrt{4\pi Dt}} \exp\left[-\frac{x^2}{4Dt}\right], \quad t \ll t_a, \quad (29)$$

$$c(x, t) \approx \frac{1}{2\Gamma(\frac{1}{4})} \sqrt{\frac{t_a}{t}} \frac{N_0}{\sqrt{D\sqrt{t_a t}}} \left[1 - \frac{\Gamma^2(\frac{1}{4})}{8\pi\sqrt{2}} \alpha^2\right], \quad (30)$$

$$\alpha \ll 1, \quad t_a \ll t \ll t_b$$

$$c(x, t) \approx F_3(x, t) = \sqrt{\frac{t_a}{t_b}} \frac{N_0}{\sqrt{4\pi\tilde{D}t}} \exp\left[-\frac{(x - \tilde{u}t)^2}{4\tilde{D}t}\right], \quad (31)$$

$$t \gg t_b$$

where

$$\tilde{D} = D \sqrt{\frac{t_a}{t_b}}, \quad \tilde{u} = u \sqrt{\frac{t_a}{t_b}}. \quad (32)$$

Fig. 12 shows numerical simulation results and asymptotics F_3 for various time moments t and characteristic times t_a and t_b . It can be observed that for the selected parameters the propagating admixture concentration wave has a symmetric form, and its amplitude drops with reduction of the ratio t_a/t_b , while the wave velocity also drops with reduction of the ratio t_a/t_b .

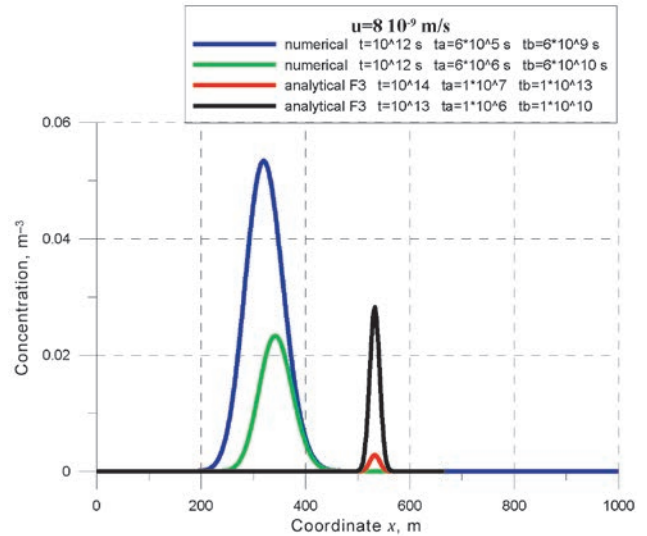


Fig. 12. Numerical and analytical (asymptotics F_3) concentration distribution profile for various time moments t and characteristic times t_a and t_b

2 Application of the two-porous environment model to migration of radionuclides at the "Eniseyskiy" site of Nizhnekansk massif

Adequate application of the developed numerical and analytical methods requires, first of all, identification of the main input parameters of the model. This requires geological investigations to be carried out, including both direct methods (drilling works; investigation of kerns in order to obtain porosity, fracture, permeability and saturation parameters; hydrogeological studies at the surface and at deep levels, etc.) and indirect methods (geophysical studies, identification of water age, study of stress-deformed condition, studies of similar rocks, etc.).

A certain amount of such works has already been completed at the "Eniseyskiy" site. In particular, the main hydrogeological parameters were measured, as well as porosity and fracture measurements. Of course, all of these parameters will be specified in the future measurements and planned tests and experiments at the underground research laboratory.

2.1 Assessment of the main input parameters of the model

Assessment of the most important system parameters t_a and t_b requires knowledge of environment porosity φ_b and fractures φ_{fr} . The available assessments of these values are the following: $\varphi_b \sim 6 \cdot 10^{-3} - 3 \cdot 10^{-2}$, $\varphi_{fr} \sim 3 \cdot 10^{-3}$ [1].

Parameter A is the ratio of block porosity to fractures (volumetric fraction taken by mobile subareas):

$$A = \varphi_b / \varphi_{fr}. \quad (33)$$

If the upper range boundary is taken as the true value, then the parameter A is approximately equal

to 10 and, correspondingly, the ratio of characteristic times in the problem would be equal to

$$\frac{t_a}{t_b} = \frac{1}{A^2 R^2} \approx 10^{-4} - 10^{-2} \quad (34)$$

dependent on retardation factor R due to sorption. As mentioned above, it is assumed that it is varied in the range from 1 (unabsorbed admixtures) to 16 (strongly adsorbed admixtures).

In this case t_b is assessed as

$$t_b = \left(\frac{V_b}{S_b} \right)^2 \frac{R}{d} \approx 10^{11} - 10^{12} \text{ s.} \quad (35)$$

In assessment (35) characteristic block dimension V_b/S_b was taken to be in the range between 3 and 10 m, while diffusion coefficient in blocks (10) was equal to $d \approx 10^{-10} \text{ m}^2/\text{s}$.

2.2 Results of analytical and numerical modeling for the "Eniseyskiy" site

Advection rate is required for calculations - representing the velocity in the mobile subsystem for the Nizhnekansk massif in the vicinity of radioactive waste disposal facility (RWDF). Effective filtration rate and true mass transport rate was assessed in report [1].

True mass transport (advection) rate for hydrogeological mode of the underground water in the vicinity of RWDF was

$$u = L/t_0 \approx 5500/2200 \approx 0,25 \text{ m/year} = 8 \cdot 10^{-9} \text{ m/s.} \quad (36)$$

Here L – length of flow line towards the Enisey River, m, t_0 – lifetime of the simulated particle in the massif.

Let us consider quasi-single dimensional admixture migration towards the river (Fig. 13). Results of numerical modeling for various input parameters are given in Fig.14, while the analytical results (asymptotics F_3) are shown in Fig. 15. The results demonstrate that the effective transport rate of particle cloud is strongly dependent on characteristic times of the problem t_a and t_b . Let us bear in mind that these parameters also include sorption parameter R , while the ratio t_a/t_b is reversely proportional to R .

Let us return to the conclusions of it.1.2, equations (31), (32). Effective concentration wave propagation rate is equal to

$$u_{eff} = \tilde{u} = u \sqrt{\frac{t_a}{t_b}} \approx 10^{-10} \text{ M/c.} \quad (37)$$

Therefore, the characteristic time for the admixture (with low sorption capability $R \approx 1$, for example, ¹²⁹I) to reach Enisey River, would be of the order of $\tau \approx L/u_{eff} \approx 10^{15} \text{ s} \approx 300\,000 \text{ years}$ for $t_a/t_b = 10^{-4}$. If the admixture would propagate towards the Shumikha

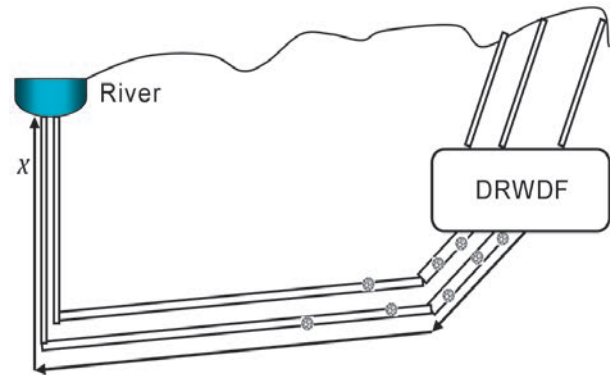


Fig. 13. Schematic presentation of the geometry of admixture migration towards the river problem

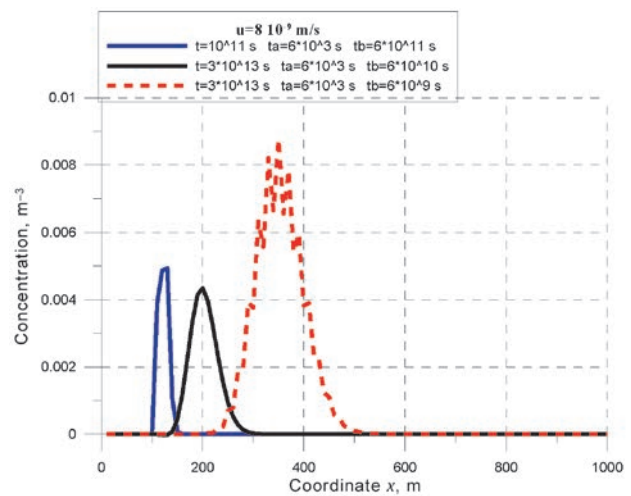


Fig. 14. Numerical concentration distribution profile in logarithmic scale for various time moments t and characteristic times t_a and t_b

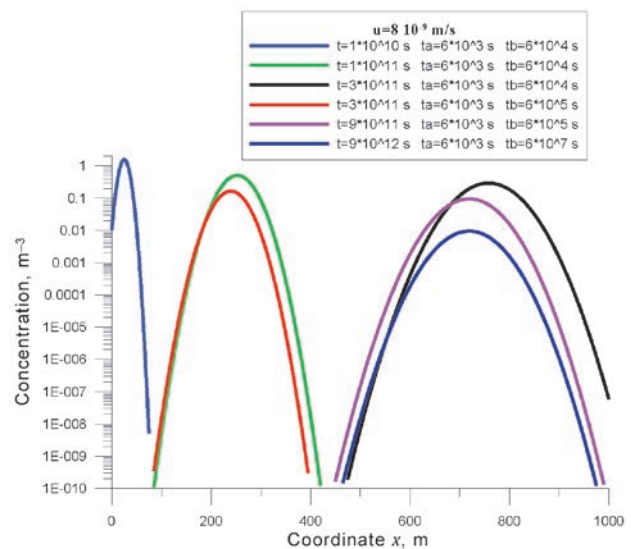


Fig. 15. Asymptotic concentration distribution profile in logarithmic scale for various time moments t and characteristic times t_a and t_b

River, the time for the particles to reach the River would be approximately equal to 100 000 years for the same advection rate. For radionuclides with high sorption capability $R \gg 1$ (for example, ^{135}Cs) these would be even higher by R times, where R – retardation factor for sorption of this isotope.

However, amplitude (maximum) of the concentration wave reaching the river would depend on the ratio t_a/t_b . This amplitude would be equal to the value derived from equation (31), with account for expression for migration time τ :

$$B \approx \sqrt{\frac{t_a}{t_b}} \frac{N_0}{\sqrt{4\pi\tilde{D}\tau}} = \sqrt{\frac{t_a}{t_b}} \frac{N_0}{\sqrt{4\pi\tilde{D}\tau \sqrt{\frac{t_a}{t_b}}}} = \frac{N_0}{\sqrt{4\pi\tilde{D}\tau}} \left(\frac{t_a}{t_b}\right)^{1/4} \quad (38)$$

or with account for assessment for τ :

$$B \approx \frac{N_0 \sqrt{u}}{\sqrt{4\pi DL}} \left(\frac{t_a}{t_b}\right)^{3/4}$$

Amplitude is reversely proportional to the square root of the migration pathway length for the constant ratio t_a/t_b . For example, for unitary concentration at the disposal location, concentration at the release point to daylight surface would reach about $3 \cdot 10^{-5}$ for time moment τ corresponding to the time the nuclides would reach riverbed of the Shumikha or the Enisey and for $t_a/t_b = 10^{-4}$.

The area under the curve, i.e. the number of particles in the fast environment would be equal to

$$B \sqrt{4\tilde{D}\tau} = \frac{N_0}{\sqrt{\pi}} \left(\frac{t_a}{t_b}\right)^{1/2}, \quad (39)$$

i.e. would be independent of time. It should be this way, as for high characteristic times ($t \gg t_a, t_b$) the blocks would be already filled with admixture. This statement is in agreement with (18), i.e. the number of particles in the mobile environment is constant and is equal to N_2 .

The applicability of quasi-singledimensional approximation for the problem of admixture migration towards the river is confirmed by the characteristic diffusion blurring of admixture concentrations in the directions of y and z axis:

$$\delta \approx \sqrt{\tilde{D}\tau} \approx 10 \text{ m},$$

i.e. is significantly lower than the characteristic dimensions of the problem.

Another consequence of expression (39) is that the number of particles reaching the river (Enisey or Shumikha) is proportional to the square root of the ratio t_a/t_b . Parameter ratio t_a/t_b is clearly defined by geometric properties. This means that the possible changes in the number of particles in the wave reaching the river are connected to changes of such parameters as porosity, fractures, distribution

of fracture dimensions or sorption capabilities of particles.

The most important radionuclides from the point of view of environmental impact are listed in table 3. Literature analysis showed that there are experimental transport data available for many nuclides, which would need to be supplemented by the results of tests at future URL site. Thus, nearly all isotopes listed in the table, with the exception of low activity isotopes ^{238}U , ^{135}Cs and ^{129}I , would decay by the time they reach the daylight surface.

Table 3. The most important radionuclides, their half-lives and maximum allowed specific activities as components of RW in packages sent for disposal

Radio-nuclide	Half-life $T_{1/2}$, years	Maximum allowed specific activities as components of RW in packages sent for disposal at DRWDF, Bq/kg
^{129}I	$1,57 \cdot 10^7$	$4,4\text{E}+03$
^3H	$1,24 \cdot 10^1$	$2,3\text{E}+08$
^{99}Tc (TcO_4^-)	$2,13 \cdot 10^5$	$5,1\text{E}+06$
^{79}Se (SeO_3^{2-})	$6,50 \cdot 10^4$	$4,5\text{E}+04$
^{90}Sr	$2,91 \cdot 10^1$	$5,6\text{E}+08$
^{238}U	$4,47 \cdot 10^9$	$2,1\text{E}+05$
^{137}Cs	$3,00 \cdot 10^1$	$1,3\text{E}+09$
^{135}Cs	$2,30 \cdot 10^6$	$6,0\text{E}+04$
^{243}Am	$7,38 \cdot 10^3$	$2,1\text{E}+05$
^{239}Pu	$2,41 \cdot 10^4$	$8,3\text{E}+07$

In conclusion let us look in detail at the simulation of boundary condition at the point of radionuclides release to the river. Zero boundary condition looks advisable, i.e. $c(x=L)=0$. As the correlation $F_3(x, u, t)$ has zero value at infinity $F_3(\infty, u, t)=0$, then the boundary condition $c(x=L)=0$ would be satisfied by the following combination (Fig. 16):

$$F_3(x, u, t) + F_3(-x, -u, t).$$

This means that the admixture flow at the point of release to the river is equal to

$$-D \frac{\partial c}{\partial x} \Big|_{x=L} + u c \Big|_{x=L} = 2 \left(-D \frac{\partial F}{\partial x} \Big|_{x=L} + u F \Big|_{x=L} \right),$$

i.e. the real flow is doubled due to image compared to the asymptotics F_3 .

Overall, the obtained results for characteristic times of radionuclide release to daylight surface are one-two orders of magnitude higher compared to the results of report [1].

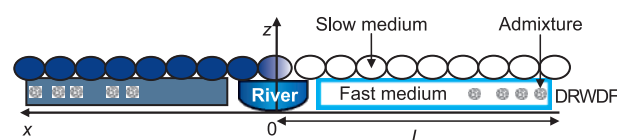


Fig. 16. Illustration of the image method for the problem of admixture migration from DRWDF towards the river

Conclusion

Numerical simulation of admixture diffusion and advection for quasi single-dimensional case was carried out. The available values of the main characteristics of hydrogeological environment for the “Eniseyskiy” site of Nizhnekansk massif were used as input parameters for the model. The results obtained show reasonable physical behaviour for the most interesting spatial areas (near field, near distribution tail, far distribution tail).

Asymptotics F_0 and F_1 (for the case of diffusion) and F_2 and F_3 (for the case of advection) provide very good approximation for the numerical solutions of the admixture transport problem in two-porous environment. Function F_0 describes the near field, functions F_1 and F_2 approximate the near tail of the distribution, and the function F_3 is applied for assessment of the far tail of distribution. Reasonable agreement of the numerical simulation and asymptotic analysis results was obtained in the calculations.

Asymptotic analysis is a powerful tool for study of transport processes. It provides good assessments of key output parameters for solution of classic and non-classic transport problems, and has a number of advantages specifically for the problem of study of radionuclide migration for large distances from the source.

Water saturated rock massif of the “Eniseyskiy” site is a natural barrier preventing radionuclide transport by delaying their migration and reducing the concentration at the points of release to the daylight surface.

Preliminary assessments based on numerical modeling results and asymptotic analysis lead to a conclusion that radionuclides with low sorption capability will reach the Enisey River riverbed in time of the order $3 \cdot 10^5$ – $1 \cdot 10^6$ years after the failure of safety barriers. For radionuclides with high sorption capability this time will be even longer by R times, where R — retardation factor for sorption capability. At the same time, the transport mode will change both in the general plume and in the near and far tails in the following sequence: first classic mode, then non-classic mode (subdiffusion), and, finally, classic behavior again, but with a reduced advection rate.

There are grounds to suppose that due to such long radionuclide migration times, their impact at the points of release to daylight surface would be insignificant and below threshold values.

Acknowledgements

The authors express the deep gratitude to IBRAE associates A. S. Barinov and S. A. Bogatov for materials provided and the fruitful remarks during discussions.

This work was partly supported by the Russian Foundation for basic research (project no. 18-08-01229).

References

1. Otchet po obosnovaniyu bezopasnosti deyatelnosti po razmeshcheniyu i sooruzheniyu ne otnosyashchegosya k yadernym ustanovkam punkta khraneniya RAO, sozdavayemogo v sootvetstvii s proyektnoy dokumentatsiyey na stroitelstvo obyektov okonchatelnoy izolyatsii RAO (Krasnoyarskiy kray. Nizhnekanskiy massiv) v sostave podzemnoy issledovatel'skoy laboratorii. Glava 6. Radiatsionnaya bezopasnost. — Moskva, FGUP “NO RAO”, 2015. — S. 6-1—6-382. (In Russian).
2. Barenblatt G. I., Zheltov Yu. P., Kochina I. N. Ob osnovnykh predstavleniyakh teorii filtratsii odnorodnykh zhidkostey v treshchinovatykh porodakh. Prikladnaya matematika i mekhanika, 1960, t. 24, vyp. 5. (In Russian).
3. Gerke H. H., van Genuchten M. Th. A Dual-Porosity Model for Simulating the Preferential Movement of Water and Solutes in Structured Porous Media. Water Resour. Res., v. 29, 1993, p. 305.
4. Rumynin V. G. Geomigratsionnyye modeli v gidrogeologii. — SPb.: Nauka. 2011. — 1160 c. (In Russian).
5. Havlin S. and Ben-Avraham D. Adv. Phys., v. 36. 1987. p. 695.
6. Bouchaud J.-P. and Georges A. Phys. Rev., v. 195, 1990, p. 127.
7. Isichenko M. B. Rev. Mod. Phys., v. 29, 1992, p. 961.
8. Dentz M., Borgne T. L., Englert A. et al. J. Contam. Hydrol., v. 120-121, 2011, p. 1.
9. Matveyev L. V. Perenos primesi v treshchinovoporistoy srede s sorbtsiyey. ZhETF, t. 142, vyp. 5 (11), s. 943—950.
10. Pruess K., Narasimhan F. N. On Fluid Reserves and the Production of Superheated Steam from Fractured Vapor Dominated Geothermal Reservoirs. Journal of Geophysical Research, v. 87, 1982, No B11, pp. 9329—9339.
11. Pruess K. A Mechanistic Model for Water Seepage through Thick Unsaturated Zones in Fractured Rocks of Low Matrix Permeability. Water Resources Research., v. 35, 1999, No 4, pp. 1039—1051.

Information about the authors

Vasiliev Alexander Dmitrievich, Ph.D., senior research associate, Nuclear Safety Institute of RAS (52, Bolshaya Tulkaya st., Moscow, Russia, 115191), e-mail: vasil@ibrae.ac.ru.

Kondratenko Petr Sergeevich, Professor, head of laboratory, Nuclear Safety Institute of RAS (52, Bolshaya Tulkaya st., Moscow, Russia, 115191), e-mail: kondrat@ibrae.ac.ru.

Matveev Leonid Vladimirovich, Professor, acting director, Nuclear Safety Institute of RAS (52, Bolshaya Tulkaya st., Moscow, Russia, 115191), e-mail: matveev@ibrae.ac.ru.

Bibliographic description

Vasiliev A. D., Kondratenko P. S., Matveev L. V. Nonsteady-State Model of Double Porosity for the Consideration of Radionuclides' Migration at the “Eniseyskiy” Site. Radioactive Waste, 2018, no 1 (2), pp. 76—88.